LEO satellite imaging with adaptive optics

Cyril Petit, Laurent Mugnier, Vincent Michau, Joseph Montri, Bruno Fleury

LEO SATELLITE IMAGING WITH ADAPTIVE OPTICS

C. Petit *[a], L. Mugnier[a], V. Michau[a], J. Montri[a], B. Fleury[a]
[a] DOTA/Onera, Paris Saclay University, 92322 Châtillon, France.

ABSTRACT

Space Situational Awareness (SSA) has become a key issue both for defense and civilian/industrial applications. Identification of potential or active threats and monitoring of key assets and operations are at stake. But it also includes follow up of dedicated satellites (such as telecommunication, observation), traffic handling, debris identification and tracking. Radar imaging is not enough for detailed characterization and identification of satellites, even for low earth orbits, and optical imaging can provide a powerful and complementary tool. We present current works performed at Onera on adaptive optics for Low Earth Orbit (LEO) satellite imaging. We briefly present our system and focus on the specific developments made to tackle the particular issue of fast moving targets observed through the atmosphere. We also discuss image post-processing in this particular framework, where turbulence conditions and correction strongly evolve along the observation, leading to a badly known point spread function (PSF). We have developed a robust and efficient post-processing method based on recent works for both astronomical and biomedical observations. We discuss further possible improvements.

Keywords: Adaptive optics, satellite imaging

1. INTRODUCTION

Recent announcements emanating for instance from the United States of America or France, have shown that space is now an explicit part of national defence strategies. As such, monitoring of key assets, control of operations such as satellite posting and identification of potential or active threats are required, from Low Earth Orbit (LEO) to Geosynchronous Earth Orbit (GEO) orbits. These issues not only matter for National Defence. It may also be of particular interest for civilian applications, such as monitoring of dedicated satellites (telecommunication, observation, and scientific missions), traffic handling, debris identification and tracking. LEO orbits are particularly concerned with an increasing number of satellites occupying this space. Trajectories can be easily tracked thanks to radar detection, while radar imaging can provide identification of satellites, though with limited resolution and in-depth imaging [1]. Optical imaging can provide complementary high resolution images and assessment of the identity, status, dynamics of a satellite and control of its vicinity. This requires large aperture telescopes with fast steering capabilities to track fast moving targets. Adaptive Optics (AO) is then required to compensate for atmospheric turbulence. The USA has thus developed state-of-the-art assets in this prospect [2][3]. The goal of this paper is to present and discuss the results obtained with a dedicated prototype. We also present innovative works for image post-processing in this particular framework.

Onera has indeed developed for the French Defence Agency a prototype of Adaptive Optics (AO) assisted imager of LEO satellites. The AO bench is located on the MeO telescope of the Observatoire de la Cote d'Azur (OCA) and presents by construction limited capabilities, in particular regarding temporal aspects. We have thus developed a GPU-CPU based real time controller to reduce loop delay and thus temporal error. This controller also provides the flexibility to consider partial automation as an answer to fast evolving conditions. Considering satellite imaging, post-processing is also a key issue. We have thus developed dedicated blind deconvolution algorithms taking advantage of recent works performed in astronomy and biomedical imaging. We first describe briefly the AO system and focus on the temporal limitations. We describe the technological upgrades performed to increase the AO performance. We then discuss post-processing and current results obtained on a civilian LEO satellite.

* *cyril.petit@onera.fr*

2. METHODS AND MATERIALS

The AO system, called ODISSEE, is located on the MeO telescope of OCA. The MeO telescope and the AO system have been partly described in the framework of tests for satellite-to-ground optical telecommunication [4]. We summarize the main features and limitations of the set-up.

2.1 Experimental set-up

The MeO station is a versatile telescope located in the hinterland of Grasse at an altitude of 1270 meters, up to now mostly used for artificial satellites and lunar laser ranging. This 1.5-meter telescope (Fig. 1) is installed on an Alt-Az mount allowing target tracking up to 5°/s, with a better than 20" Peak-Valley (PV) pointing accuracy thanks to a two-stage dedicated tracking loop. These features make this telescope a very good candidate for various research programs such as optical time transfer, adaptive optics, high resolution imaging, debris detection, optical telecom and astronomical observation.

Fig. 1 Picture of MeO telescope.

The ODISSEE AO bench (Fig. 2) has been designed and integrated by ONERA at the coudé focus of MeO for investigation of various applications, including visible imaging. In this prospect, it has been adapted from an existing laboratory AO bench, favoring versatility rather than performance. As a consequence, this AO system is not currently designed for the typical turbulent conditions encountered at OCA. However, it provides a useful tool to assess propagation conditions and the performance of new concepts, and to investigate the limitations of AO for imaging applications.

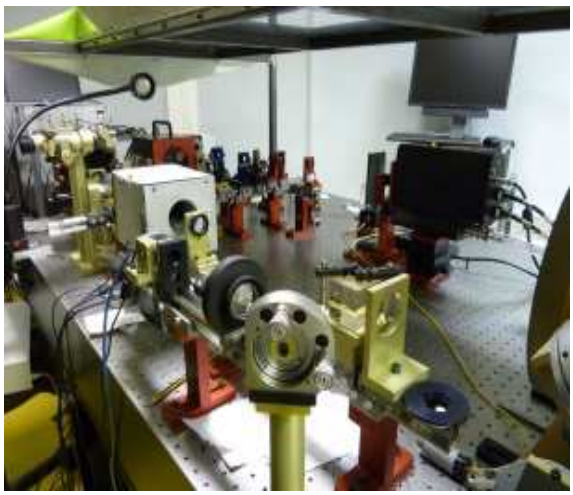

Fig. 2 Picture of ODISSEE AO bench.

The light from MeO coudé focus enters the bench at the bottom-right of the image. The AO bench includes a pupil derotator, an atmospheric dispersion compensator, a pupil stabilizer, a fast tip/tilt mirror to compensate for atmospheric turbulent tip/tilt, pointing residuals and vibrations, an 88 actuator deformable mirror, a Shack-Hartmann based wavefront sensor and an imaging camera.
ODISSEE uses a visible Shack-Hartmann WaveFront Sensor (SH-WFS) with 8x8 square sub-apertures. The field of each sub-aperture covers 30x30 pixels in the focal plane. The WFS camera is a First Light Imaging OCAM² camera (Electron Multiplying Charge Coupled Device--EMCCD) with an engineering grade E2V chip of 240x240 pixels. Slopes and intensities per sub-aperture are recorded with a frame rate of 1500 Hz. High order correction is performed thanks to a CILAS piezo-stacked Deformable Mirror (DM) with 88 actuators (10x10 cartesian grid), though the useful aperture covers only a 9x9 actuator area of the DM. All actuators are used for real-time correction. It provides a +/-5 µm mechanical stroke and exhibits a 10 kHz bandwidth.
The AO loop is controlled thanks to a Linux Personal Computer (PC) Real-Time Controller (RTC), developed by Shakti Company, implementing various possible features both in terms of wavefront sensing and control algorithms. As a baseline, a simple integrator is used. The RTC in its initial configuration exhibits only a 50Hz bandwidth, defined as the 0-dB error transfer function cut-off frequency. This leads to limited performance considering LEO imaging or optical telecommunication, which can be also easily affected by vibrations for instance.
The internal performance of the AO bench in this configuration (defined as Strehl Ratio of a non-resolved source at the entrance focus) is 88% at 850 nm (representing the ultimate performance of the system on sky), due to residual aberrations (high order residuals and non-common path aberrations).

2.2 System limitations and upgrade

Considering the MeO telescope location, the ODISSEE AO bench is clearly sub-optimal for the average turbulence conditions (seeing usually larger than 1''), with its 8x8 sub-apertures and matching DM configuration. Still, considering LEO satellite imaging or optical telecommunication, fast motion targets shall be considered. With a slew rate as high as 1°/s for LEO satellites at some 650km altitude, apparent wind velocity easily reaches 100m/s at a 10km altitude and for a 60° elevation. This leads to a very strong influence of temporal error aggravated by our slow system. Error budget analysis shows that the contribution of the temporal error is predominant as long as the AO bandwidth is not higher than 100Hz for small systems (in terms of linear actuators across the pupil) and 200Hz for larger ones (more than 12 linear actuators), which means sampling frequencies typically higher than 1500Hz and 3 kHz respectively. Temporal error is a show-stopper that shall be dealt with prior to any increase of the number of degrees of freedom, as the temporal error will increase with the number of corrected modes. We could add that, increasing the number of linear number of actuators across the pupil (and thus the number of sub-apertures) would also mean increased computation time, usually degrading the control loop delay and thus reducing the AO cut-off frequency. This leads to a second penalty for temporal error.
In order to reduce the temporal error, a GPU-CPU based RTC has been developed. This evolution leads to a drastic reduction of computation time, through a cost effective and simple software implementation as discussed in [5] and tested for instance in [6]. Our implementation allows to directly transfer the pixels from the OCAM² camera to the GPU, through a Matrox frame grabber. All wavefront sensing computations are performed by the GPU, while control and system optimization are performed by the CPU. An NVIDIA GeForce 1060 GPU board has been used, combined to low latency Ubuntu operating system. As a result, a 2.2 frame overall loop delay at 1.5kHz is obtained (70µs RTC pure delay), leading to almost 100Hz cut off frequency. This performance has been checked in the lab and on sky, through the direct estimation of the rejection (error) transfer function following method used on SPHERE [7]. Fig. 3 shows a typical experimental estimation of the transfer function on sky with an integral controller (gain set to 0.5), compared to theory with a 2 or 2.2 frame delay. This first implementation still allows significant additional gains in the future. Only 64 out of the 1700 cores of the GPU board are actually used. Increasing the number of sub-apertures thus could be done without further increase of computational delay. In addition, part of the computations is still performed on CPU. We are currently considering transferring part of control computation to the GPU or starting computations as soon as the first pixels arrive.

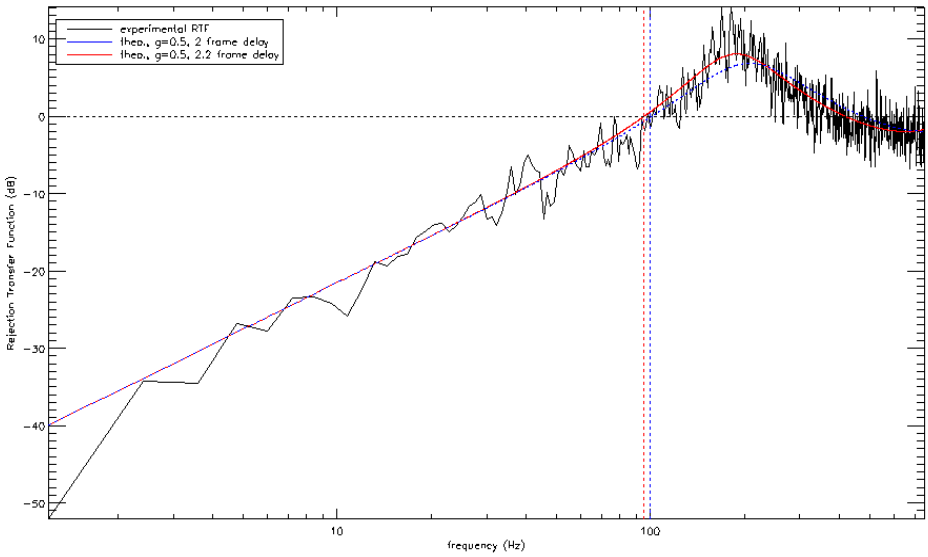

Fig. 3 Rejection transfer function of the AO system as estimated on sky (solid black), and theoretical functions for 2 (blue) and 2.2 (red) frame overall delay, same gain.

While this evolution provides limited gain on stars, the gain in performance on LEO satellite is significant and allows to reach a diffraction limited regime.
This acceleration of the real-time pipeline also allows introducing partial automation of the AO loop. Conditions strongly evolve along the observation: slew rate and SNR due to satellite distance, turbulent profile and thus apparent seeing due to elevation. For all these reasons, the AO loop optimal parameters should evolve rather quickly, without human real time intervention. The gain in real time control delay has allowed us to implement background and noise automatic follow up, as well as automatic target detection. The Shack-Hartmann wavefront sensing optimization has been fully automated, including the online adjustment of EMCCD gain. An adaptive control is now considered.

2.3 Post-processing

In LEO satellite imaging as in many imaging modalities, the image can be modelled as the noisy convolution of the sought object with a PSF that is unknown, both because a recorded star image would bear little resemblance with the actual PSF of a fast-moving satellite and because the WFS measurements would yield a noisy and low-resolution version of the actual PSF. The conventional way of tackling this lack of knowledge is to perform a “blind” or “myopic” deconvolution, consisting in a joint estimation of the sought object and of the PSF, if possible with additional constraints such as PSF band-limitedness and positivity, object positivity and support, etc (see [8] for a review). Without positivity or object support constraints the blind deconvolution has been shown to be degenerate for a quadratic regularization [9], in the sense that the estimation leads to a wrong (object, PSF) couple even if the noise level is arbitrarily small. And we have checked by simulations that even with the positivity constraint and a non-quadratic regularization, the problem remains degenerate in practice.

The problem fundamentally lies in the fact that there are too many unknowns for too little data, and the idea for a solution is twofold. Firstly, we use a parsimonious PSF model tailored for AO-corrected PSFs in order to reduce the number of unknowns [10]. Secondly, we identify the PSF by “estimating the PSF only”, on average for all possible objects within a given class; then we deconvolve the image in a non-blind fashion with the identified PSF. Fig. 4 shows the workflow of the deconvolution procedure. The above idea of estimating only the PSF is embodied in the so-called marginal blind deconvolution [9] used in this communication, where the likelihood is marginalized over the unknown object (of a given Power Spectral Density (PSD)), and maximized as a function of the sole PSF. Finally, because the PSDs of the object and of the noise are actually unknown, we must also estimate them. To this purpose, we also use a sparse parameterization for the object’s PSD with only three parameters [11], so that the statistical contrast of our estimation (ratio of number of data over the number of unknowns) remains much greater than unity, and the appealing theoretical properties of Maximum Likelihood estimation such as consistency are retained in practice.

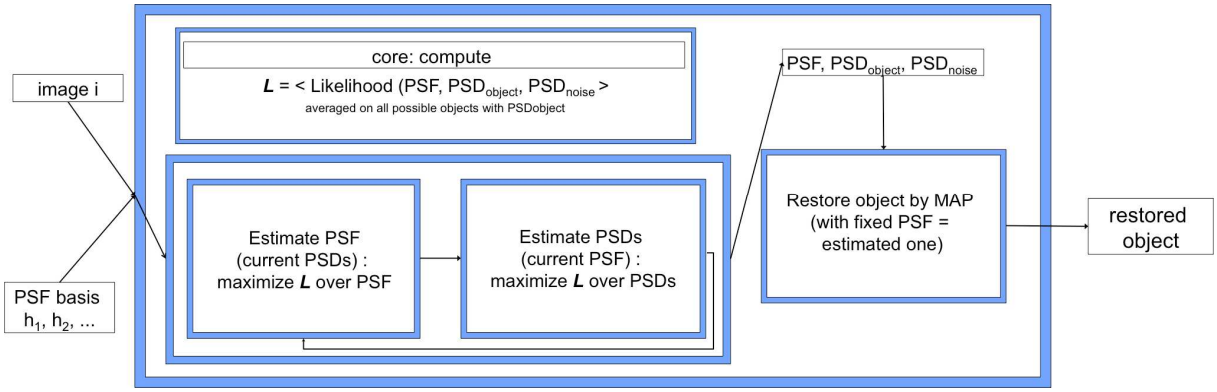

Fig. 4 Sketch of the deconvolution procedure.

3. RESULTS

Although the analysis of on-sky performance will not be detailed here, some images with AO correction are shown. The imaging of the ENVISAT satellite has been performed and is presented below. ENVISAT (Fig. 5) is an ESA satellite, launched in 2002, and dedicated to Earth observation through radar and spectrometry. This is a large satellite (26m long with its solar panels) evolving at some 800km altitude. However, this satellite is no more controlled, since 2012, and represents today the largest space debris in orbit. It has been observed by CNES through the Pleiades space telescope and by TIRA Inverse Synthetic Aperture Radar imager (Fraunhofer institute) [12] in order to provide a long-term analysis of the satellite rotation, in the prospect of a possible de-orbitation program led by ESA.

Fig. 5 Picture of ENVISAT

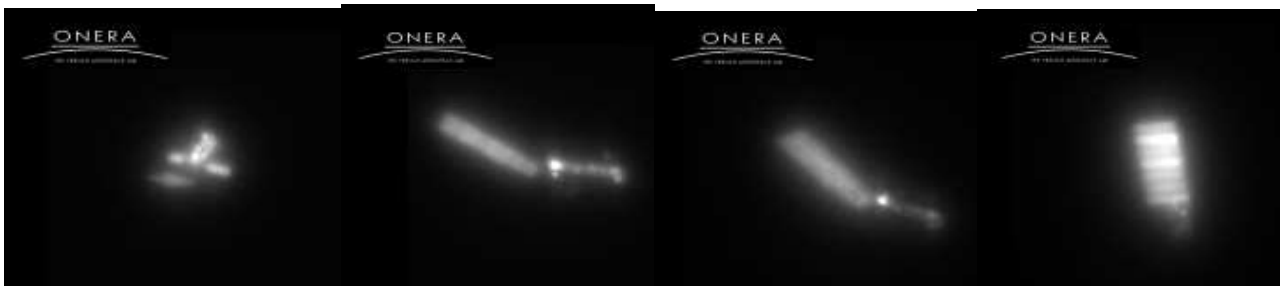

Fig. 6 Series of AO corrected images of ENVISAT**.**

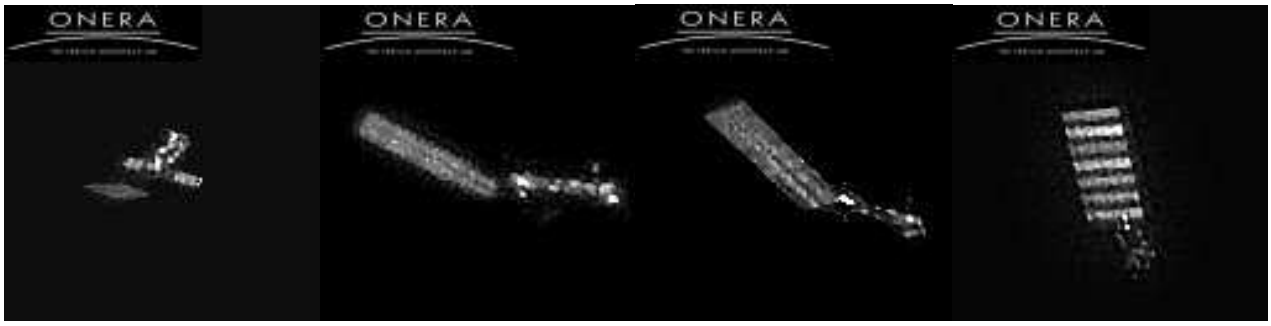

Fig. 7 Series of AO corrected images of ENVISAT after post-processing.

Fig. 6 shows AO corrected images of ENVISAT taken from a sequence of a few minutes. The satellite rotation is clearly visible along the sequence, as illustrated in these few snapshots, as well as some structural details.
Application of post-processing can then help restore the object and significantly increase the image quality, as shown in Fig. 7. These images can be compared to ISAR images as shown in [12].

4. CONCLUSION

While the current AO system is clearly sub-optimal with respect to the turbulence conditions, the optimization of the real-time computation pipeline has allowed to drastically improve the final AO performance and introduce on-line optimization of the AO parameters. This represents a key asset for LEO imaging but also for optical telecommunications, so as to deal with fast evolving conditions through automated systems. Technological RTC developments shall be pursued further, as telecommunication applications tend to push sampling frequencies higher, with 5 to 10 kHz goals. In the meantime, refining the AO loop control, considering for instance predictive solutions based on Linear Quadratic Gaussian Control, could participate to the reduction of the temporal error such as in [13]. Such a control approach could then include the on-line optimization of the control parameters with respect to observing conditions, as the latter will evolve significantly during the observation.
Post-processing of AO corrected images has also been improved, both in terms of performance and robustness, thanks to marginal blind deconvolution and use of a parsimonious PSF parametrization. Further improvements can still be expected, by taking into account the AO information as well as by processing image sequences jointly.
Next steps shall focus on increasing observation opportunities. This implies firstly observing at low elevations and secondly during daytime. Indeed, satellite imaging as well as optical telecommunications are strongly limited at low elevations, due to the strong turbulence conditions. However most of the available time of visibility of a LEO satellite is below 30°, leading to a strong reduction of observation or link duration. In addition, satellite observation is limited to few hours of the night. These limitations suggest considering further improvements of AO but also considering other modalities of image post-processing as underlined by [13].

5. ACKNOWLEDGMENT

This work has been supported by the French Defense Agency under contract 2015990015. The authors are grateful to the Shakti company for the development of the real-time computer and their strong involvement in the project. The authors are also grateful to Observatoire de la Côte d'Azur for providing access to the MeO telescope, for their extensive support and long-term involvement in this project, in particular in fine tracking of satellites. Finally, the authors are grateful to R. Fétick, T. Fusco and B. Neichel for their strong contribution in particular regarding the PSF model.

REFERENCES

[1]. *Radar mappings for attitude analysis of objects in orbit*, S. Lemmens, H. Krag, J. Rosebrock, I. Carnelli, Proc. 6th European Conference on Space Debris', Darmstadt, Germany, 22-25 April 2013 (ESA SP-723)

[2]. *Starfire Optical Range 3.5-m telescope adaptive optical system*, J. M. Spinhirne, Jeff G. Allen, George A. Ameer, James M. Brown, Julian C. Christou, et al., Proc. SPIE 3353, Adaptive Optical, System Technologies, (11 September 1998)

[3]. *Characterization of the AEOS Adaptive Optics System,* L. C. Roberts, C. R. Neyman, Publications of the Astronomical Society of the Pacific, 114:1260–1266, November 2002

[4]. *Investigation on adaptive optics performance from propagation channel characterization with the small optical transponder.* Petit, C**,** Védrenne, N., Velluet, M.-T., Michau, V., Artaud, G., Samain, E., Toyoshima, M., Opt. Eng. 0001, 55(11), 2016.

[5]. *Enabling technologies for GPU driven adaptive optics real-time control,* A. Sevin, D. Perret, D. Gratadour, M. Lainé, J. Brulé, and B. Le Ruyet, Proc. SPIE 9148, Adaptive Optics Systems IV, 91482G (21 July 2014)

[6]. *The use of CPU, GPU and FPGA in real-time control of adaptive optics systems,* L.F. Rodríguez Ramos, J.J. Díaz García, J.J. Fernández Valdivia,H.M. Chulani, C. Colodro Conde, J.M. Rodríguez Ramos, Adaptive Optics for Extremely Large Telescopes 4 Proceedings, 1(1), 2015

[7]. *SAXO: the extreme adaptive optics system of SPHERE (I) system overview and global laboratory performance,* J.-F. Sauvage et al, J. Astron. Telesc. Instrum. Syst. 2(2), 2016

[8]. *Blind Image Deconvolution*, L. Blanc-Féraud, L. Mugnier & A. Jalobeanu, chap. 3 of Inverse Problems in Vision and 3D Tomography, pp. 97-121, ed. by A. Mohammad-Djafari, ISTE/John Wiley, London, 2010.

[9]. *Marginal blind deconvolution of adaptive optics retinal images*, L. Blanco and L. M. Mugnier, Opt. Express, vol. 19, pp. 23227-23239, 2011.

[10]. *Physics-based model of the adaptive-optics-corrected point spread function. Applications to the SPHERE/ZIMPOL and MUSE instruments*, R. JL. Fétick, T. Fusco, B. Neichel, L. M. Mugnier, O. Beltramo-Martin, A. Montmerle Bonnefois, C. Petit, J. Milli, J. Vernet, S. Oberti, and R. Bacon, *Astron. Astrophys.*, 628:A99, 2019.

[11]. *Myopic deconvolution of adaptive optics images by use of object and point spread function power spectra*, J.-M. Conan, L. M. Mugnier, T. Fusco, V. Michau, and G. Rousset, Appl. Opt., 37(21):4614–4622, 1998.

[12]. *Radar mappings for attitude analysis of objects in orbit*, S. Lemmens, H. Krag, J. Rosebrock, and I. Carnelli, Proc. 6th European Conference on Space Debris', Darmstadt, Germany, 22–25 April 2013

[13]. *Identification Scheme with Stability Constraints for High Velocity Turbulence in Adaptive Optics*, J. Cranney, J. De Dona, V. Korkiakoski, F. Rigaut. 2018 Australian & New-Zealand Control Conference, Swinburne University of Technology, Melbourne, Australia, Dec 7-8, 2018

[14]. *A Comprehensive Approach to High-Resolution Daylight Imaging for SSA*, M. Hart, S. Jefferies, D. Hope, J. Nagy, and R. Swindle, Advanced Maui Optical and Space Surveillance Technologies Conference (AMOS), 2016